A resetting particle embedded in a viscoelastic bath

Biswas, Arup; Dubbeldam, Johan L.A.; Sandev, Trifce; Pal, Arnab

DOI
10.1063/5.0253019

Publication date
2025

Document Version
Final published version

Published in
Chaos

RESEARCH ARTICLE | MARCH 14 2025

A resetting particle embedded in a viscoelastic bath

Special Collection: Anomalous Diffusion and Fluctuations in Complex Systems and Networks

Arup Biswas ; Johan L. A. Dubbeldam ; Trifce Sandev ; Arnab Pal

Chaos 35, 031102 (2025)
https://doi.org/10.1063/5.0253019

Chaos ARTICLE pubs.aip.org/aip/cha

A resetting particle embedded in a viscoelastic bath

Cite as: Chaos 35, 031102 (2025); doi: 10.1063/5.0253019
Submitted: 13 December 2024 · Accepted: 14 February 2025 ·
Published Online: 14 March 2025

Arup Biswas,[1,a] Johan L. A. Dubbeldam,[2,b] Trifce Sandev,[3,4,5,c] and Arnab Pal[1,d]

AFFILIATIONS

[1]The Institute of Mathematical Sciences, CIT Campus, Taramani, Chennai 600113, India and Homi Bhabha National Institute, Training School Complex, Anushakti Nagar, Mumbai 400094, India
[2]Delft Institute of Applied Mathematics, Delft University of Technology, 2628 CD Delft, The Netherlands
[3]Research Center for Computer Science and Information Technologies, Macedonian Academy of Sciences and Arts, Bul. Krste Misirkov 2, 1000 Skopje, Macedonia
[4]Institute of Physics, Faculty of Natural Sciences and Mathematics, Ss. Cyril and Methodius University, Arhimedova 3, 1000 Skopje, Macedonia
[5]Department of Physics, Korea University, Seoul 02841, South Korea

Note: This paper is part of the Focus Issue on Anomalous Diffusion and Fluctuations in Complex Systems and Networks.
[a]**Electronic mail:** arupb@imsc.res.in
[b]**Electronic mail:** J.L.A.Dubbeldam@tudelft.nl
[c]**Electronic mail:** trifce.sandev@manu.edu.mk
[d]**Author to whom correspondence should be addressed:** arnabpal@imsc.res.in

ABSTRACT

We examine the behavior of a colloidal particle immersed in a viscoelastic bath undergoing stochastic resetting at a rate r. Microscopic probes suspended in a viscoelastic environment do not follow the classical theory of Brownian motion. This is primarily because the memory from successive collisions between the medium particles and the probes does not necessarily decay instantly as opposed to the classical Langevin equation. To treat such a system, one needs to incorporate the memory effects into the Langevin equation. The resulting equation formulated by Kubo, known as the generalized Langevin equation (GLE), has been instrumental to describing the transport of particles in inhomogeneous or viscoelastic environments. The purpose of this work, henceforth, is to study the behavior of such a colloidal particle governed by the GLE under resetting dynamics. To this end, we extend the renewal formalism to compute the general expression for the position variance and the correlation function of the resetting particle driven by the environmental memory. These generic results are then illustrated for the prototypical example of the Jeffreys viscoelastic fluid model. In particular, we identify various timescales and intermittent plateaus in the transient phase before the system relaxes to the steady state; and further discuss the effect of resetting pertaining to these behaviors. Our results are supported by numerical simulations showing an excellent agreement.

The diffusion process of a colloidal particle or a polystyrene bead immersed in a fluid such as water is a cornerstone in statistical physics. If the surrounding fluid molecules are smaller and faster than the probe, a distinct separation of timescales can be observed, which results in a dynamics that is Markovian or memoryless in nature. It is well known that such dynamics can be described by the celebrated Langevin equation. Nonetheless, this is no longer the case when the probes are driven through solutions in the presence of long macromolecules, a dense environment, or a viscoelastic medium. Such dynamics are more complex, giving rise to memory effects, and are quantified by the generalized Langevin equations (GLEs). We aim to study the GLE under stochastic resetting dynamics, which has emerged as a powerful mechanism to stabilize the system by eliminating the wandering-off or kinetically trapped trajectories. Our analysis reveals that resetting not only induces a stationary state into the system but also allows one to harness the timescales arising from the memory effect. Our research opens the door to designing resetting based

strategies to explore non-equilibrium transport phenomena in complex fluids.

I. INTRODUCTION

The classical theory of Brownian motion describes, for example, the random motion of a massive particle immersed in a fluid, as it was observed by Robert Brown in 1827 with pollen grains and dust particles in water. The random motion of the particle occurs due to the thermal motion of the molecules in the liquid, and the mass of the latter is much smaller than the mass of the suspended particle. Paul Langevin explained this motion of the Brownian particle with mass m by Newton's second law for a test particle in the presence of viscous dynamic friction $-\gamma_f v(t)$, deterministic external potential $V(x)$, and an internal random force $\xi(t)$, i.e.,[1]

$$m\dot{v}(t) + \gamma_f v(t) + \frac{dV(x)}{dx} = \xi(t), \quad \dot{x}(t) = v(t), \tag{1}$$

where $x(t)$ and $v(t)$ are the particle displacement and particle velocity, respectively, and γ_f is the friction coefficient. The internal force $\xi(t)$ is the Gaussian random force of zero mean ($\langle \xi(t) \rangle = 0$) and correlation $\langle \xi(t)\xi(t') \rangle = 2\gamma_f k_B T \delta(t - t')$, where $\langle \cdot \rangle$ means ensemble average. This means that the noise is internal white noise and the fluctuation and dissipation in the system come from the same source. The time scale of the molecular motion is much shorter than the time scale of the motion of the Brownian particle. The resulting mean squared displacement (MSD), i.e., $\sigma^2(t) = \langle x^2(t) \rangle - \langle x(t) \rangle^2$, in the absence of external potential ($V(x) = 0$) in long time limit shows a linear time dependence, $\sigma^2(t) \sim t$, which is characteristic for normal diffusion, while at short times, the motion is ballistic due to the inertial effects. The transition from ballistic motion to normal diffusion is characterized by the characteristic time scale $1/\gamma_f$.

In many systems, the mass of the immersed particle is not necessarily much larger than the mass of the surrounding molecules of the environment, and, consequently, the time scale of the molecular motion is not very much shorter than the time scale of the motion of the suspended particle. In such cases, the Langevin equation for the Brownian motion should be modified to the generalized Langevin equation with friction memory kernel,[2–5] which is of interest to our work.

The generalized Langevin equation has been used to model anomalous diffusion by employing power-law friction memory kernel.[6–11] The anomalous diffusion is characterized by power-law dependence of the MSD on time, $\sigma^2(t) \sim t^\alpha$, $\alpha \neq 1$, which has been observed in various systems, from electron transfer within a single protein molecule,[12,13] to models of solute particle in a bath of fast solvent molecules[14] and particles in viscoelastic media.[15] The generalized Langevin equation model has been used in addition to the description of the conformational motions of proteins,[16,17] in the microscopic description of a tracer particle in a one-dimensional many-particle system with two-body interaction potential,[18] in the generalized elastic model of stochastic motion in membranes and semiflexible polymers[19] and polymer translocation,[20] to mention but a few. Here, we mention that a simple example of the emergence of exponential memory is in the model of Brownian motion in the presence of a harmonic potential, i.e., in the Ornstein–Uhlenbeck (OU) process.[21–23] In this work, we will be interested in the Jeffreys fluid model for a particle in a viscoelastic medium, which is also an example of the non-Markovian system.[24–32] In particular, the goal is to monitor the motion of a particle in such a fluid system under the resetting dynamics as will be delineated in below.

Contrary to the exhaustive analysis of various diffusion and anomalous processes governed by different (generalized) diffusion and Fokker–Planck equations for homogeneous and heterogeneous media in the presence of stochastic resetting,[33–43] there is a lack of works related to the generalized Langevin equation in the presence of stochastic resetting. In resetting processes, a moving particle is reset to its initial (or particular) location at regular or stochastic intervals. Quite interestingly, resetting has the ability to stabilize a system by repeatedly reverting it to a fixed location. This was first observed by Evans and Majumdar in simple diffusion which, in the absence of resetting is a non-stationary process, but attains stationarity as soon as resetting is introduced.[33] A similar effect has also been observed in the above mentioned models of diffusion and Fokker–Planck equations in the presence of resetting, where the system approaches a non-equilibrium stationary state (NESS),[33,34,43–48] and the relaxation dynamics to the stationary state is shown to be far from trivial.[34,49,50]

In the present work, we consider a process described by the generalized Langevin equation in the presence of Poissonian resetting. This means that the process is renewed at random times that follow an exponential distribution given by $f_R(t) = r\,e^{-rt}$, where $1/r$ is mean resetting time (i.e., r is the resetting rate) (Fig. 1). We give a detailed analysis of the MSD and correlation functions for the general form of the friction memory kernel. Then, we apply our results to a particular form of the friction memory kernel, which is used

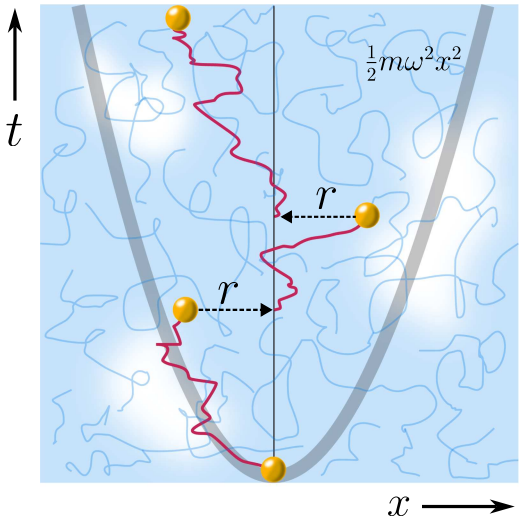

FIG. 1. Schematic representation of a colloidal particle diffusing in a viscoelastic bath under harmonic trapping. The motion of the particle is governed by the generalized Langevin equation (GLE) as in Eq. (5). In addition, the particle undergoes stochastic resetting at random time intervals drawn from an exponential distribution with mean $1/r$.

in the Jeffreys fluid model. We confirm our analytical findings by numerical simulations.

This paper is organized as follows: first (Sec. II), we discuss in detail about the generalized Langevin equation (GLE) and solve them to find the MSD and correlation function of a particle in a viscoelastic media with arbitrary kernel. Then, we elaborate on the renewal formalism of stochastic resetting in Sec. III to find the general expression for the mean and correlation function of a particle following GLE and subjected to stochastic resetting at rate r. In Sec. IV, we take the example of Jeffrey's fluid to model a viscoelastic bath to illustrate in detail about the behavior of mean and correlation function both with and without resetting. We verify our analytical findings with a numerical simulation technique, namely, the Markovian embedding scheme, as discussed in Sec. V. Finally, we conclude with a brief summary of the work and future outlook in Sec. VI.

II. GENERALIZED LANGEVIN EQUATION

Let us consider a particle of mass m in a viscoelastic bath with correlated thermal noise $\xi(t)$. Moreover, the particle is placed under a potential $V(x)$. The generalized Langevin equation (GLE) for the particle then can be written as[3,21]

$$m\ddot{x}(t) + m\int_0^t \gamma(t-t')\dot{x}(t')\,dt' + \frac{dV(x)}{dx} = \xi(t). \tag{2}$$

The quantity $\gamma(t)$ is the generalized friction kernel, which correlates the velocity of the particle at different times. In other words, this can be understood as the non-Markovian response of the particles in the fluid. The generalized fluctuation–dissipation theorem for the GLE case is given by[3,21]

$$\langle \xi(t)\xi(t')\rangle = k_B T m\gamma(|t-t'|). \tag{3}$$

Evidently, when $\gamma(t-t') = 2\gamma_f\delta(t-t')$, we recover the standard Langevin equation with a constant friction γ_f [note that, the factor 2 is canceled out from the integration in Eq. (2) as the upper limit of the integration runs upto t, which is the same point where the delta function is infinity]. The correlation, as a consequence, also takes the familiar form $\langle \xi(t)\xi(t')\rangle = k_B T m\gamma_f\delta(t-t')$. We assume the external potential $V(x)$ to be harmonic in nature so that

$$V(x) = \frac{1}{2}m\omega^2 x^2. \tag{4}$$

For the experimental conditions, in many systems, the inertial term $m\ddot{x}(t)$ in the underdamped GLE equation (2) can be neglected, which means that the friction in the system is very large. This motion is known as overdamped motion.[51] Such a case of high viscous damping (large friction) is considered to model experimental data, which are related, for example, to the movement of driven colloids in an aqueous solution of poly-ethylene oxide, which is a polymer that provides elasticity along with its inherent viscosity and renders the viscoelastic solution damped.[26,27] Similarly, due to the liquid environment of proteins, the frictional term is usually very high, and, thus, the motion of the macromolecules could be considered overdamped (see, for example, Refs. 52 and 53). Moreover, the movement within proteins is confined to a short range, and the potential can be well approximated by a harmonic potential, making the overdamped GLE for a harmonic oscillator a suitable model for the description of the dynamics within proteins.[13,52,53]

Under these assumptions, the resulting GLE in the overdamped limit takes the form

$$m\int_0^t \gamma(t-t')\dot{x}(t')\,dt' + m\omega^2 x = \xi(t). \tag{5}$$

Our aim is to analyze this overdamped GLE in the presence of stochastic resetting (Fig. 1). However, it is instructive to first revisit the techniques and solutions of GLE in the absence of resetting and find the relevant quantities of our interest. Building upon these results, we will develop methods when resetting is introduced with further elucidation of the key results.

A. GLE in Laplace space: Correlation function and MSD

We start by taking Laplace transform on both sides of Eq. (5) and dividing by m, this yields

$$\widetilde{\gamma}(s)(s\widetilde{X}(s) - x_0) + \omega^2\widetilde{X}(s) = \frac{\widetilde{\Xi}(s)}{m}, \tag{6}$$

where we denote the Laplace transformed quantities $\widetilde{X}(s) = \int_0^\infty dt\, e^{-st}x(t)$, $\widetilde{\Xi}(s) = \int_0^\infty dt\, e^{-st}\xi(t)$, $\widetilde{\gamma}(s) = \int_0^\infty dt\, e^{-st}\gamma(t)$ and $x_0 = x(t=0)$. After a slight rearrangement, one obtains

$$\widetilde{X}(s) = \left[\frac{1}{s} - \omega^2\widetilde{I}_0(s)\right]x_0 + \frac{1}{m}\widetilde{\Xi}(s)\widetilde{G}_0(s), \tag{7}$$

where the functions $G_0(t)$ and $I_0(t)$ are the so-called relaxation functions defined as

$$G_0(t) = \mathcal{L}^{-1}\left[\widetilde{G}_0(s)\right] = \mathcal{L}^{-1}\left[\frac{1}{s\widetilde{\gamma}(s) + \omega^2}\right], \tag{8}$$

$$I_0(t) = \mathcal{L}^{-1}\left[\widetilde{I}_0(s)\right] = \mathcal{L}^{-1}\left[\frac{s^{-1}}{s\widetilde{\gamma}(s) + \omega^2}\right]. \tag{9}$$

Here, the operator $\mathcal{L}^{-1}[\widetilde{f}(s)]$ stands for the Laplace inversion of the function $\widetilde{f}(s)$. Equation (7) can be inverted to write an integral solution for $x(t)$ as follows:

$$x(t) = \langle x(t)\rangle + \frac{1}{m}\int_0^t dt'\, G(t-t')\xi(t'), \tag{10}$$

where the mean position of the particle $\langle x(t)\rangle$ is given by

$$\langle x(t)\rangle = \left[1 - \omega^2 I_0(t)\right]x_0. \tag{11}$$

From Eq. (7), the correlation function in the Laplace domain is then given by

$$\langle \widetilde{X}(s)\widetilde{X}(s')\rangle = \langle \widetilde{X}(s)\rangle\langle \widetilde{X}(s')\rangle + \frac{1}{m^2}\widetilde{G}_0(s)\widetilde{G}_0(s')\langle \widetilde{\Xi}(s)\widetilde{\Xi}(s')\rangle, \tag{12}$$

where

$$\langle \widetilde{X}(s)\rangle = \left[\frac{1}{s} - \omega^2\widetilde{I}_0(s)\right]x_0, \tag{13}$$

is just the Laplace transferred mean $\langle x(t)\rangle$. The quantity $\langle \widetilde{\Xi}(s)\widetilde{\Xi}(s')\rangle$ in the above equation can be computed from Eq. (3) by performing

a double Laplace transform[54] as

$$\langle \widetilde{\Xi}(s)\widetilde{\Xi}(s')\rangle = k_B T m\left(\frac{\widetilde{\gamma}(s)+\widetilde{\gamma}(s')}{s+s'}\right). \tag{14}$$

Writing $\widetilde{\gamma}(s)$ in terms of the relaxation functions using Eqs. (8) and (9) and after simplification, we finally arrive at

$$\langle \widetilde{X}(s)\widetilde{X}(s')\rangle = \langle \widetilde{X}(s)\rangle\langle \widetilde{X}(s')\rangle + \frac{k_B T}{m}\left[\frac{\widetilde{I}_0(s)}{s'}+\frac{\widetilde{I}_0(s')}{s}-\frac{\widetilde{I}_0(s)+\widetilde{I}_0(s')}{s+s'}-\omega^2\widetilde{I}_0(s)\widetilde{I}_0(s')\right]. \tag{15}$$

The resulting correlation in the time domain, i.e., $C(t,t') = \langle x(t)x(t')\rangle$ takes the form

$$C(t,t') = \langle x(t)\rangle\langle x(t')\rangle + \frac{k_B T}{m}\left[I_0(t)+I_0(t')-I_0(|t-t'|)-\omega^2 I_0(t)I_0(t')\right]. \tag{16}$$

The MSD $\sigma^2(t) = \langle x^2(t)\rangle - \langle x(t)\rangle^2$ can be obtained by setting $t = t'$ in the correlation function so that

$$\sigma^2(t) = \frac{k_B T}{m}\left[2I_0(t)-\omega^2 I_0^2(t)\right]. \tag{17}$$

Note that we dropped the term $I_0(0)$ since from Eq. (9) and according to the initial value theorem $I_0(t=0) = \lim_{s\to\infty} s\tilde{I}_0(s) = 0$. With a specific choice of the friction kernel, one can explicitly evaluate the correlation function of a particle following GLE. We shall elaborate on the same for the Jeffreys fluid model in the later part of this article. In Sec. III, we introduce resetting to the GLE and elaborate on the theory to derive exact expressions for the MSD and the correlation function.

III. GLE WITH STOCHASTIC RESETTING

Under resetting dynamics, the motion of a particle, which follows a GLE, is intermittently stopped and the particle is brought back to the starting position $x = x_0$. This dynamics repeats itself at stochastic time intervals where the times are drawn from an exponential distribution $f_R(t) = r e^{-rt}$ with mean $1/r$ (Fig. 1). Between two consecutive resetting events, the particle follows the GLE as in Eq. (5) initiating from the same coordinate each time. Let us denote $P(x,t)$ as the probability density of the particle to be found at x at time t, starting from $x = x_0$ at $t = 0$, in the absence of resetting. Using renewal techniques,[34,43,55,56] one then can write the corresponding propagator $P_r(x,t)$ for the same system undergoing resetting as

$$P_r(x,t) = e^{-rt}P(x,t) + r\int_0^t d\tau\, e^{-r\tau}P(x,\tau). \tag{18}$$

The physical interpretation of the above equation is as follows: The first term accounts for those trajectories that did not undergo any resetting event up to time t, which occurs with a small probability e^{-rt} multiplied by the reset-free propagator $P(x,t)$. The second term on the other hand takes into account all possible trajectories, which have encountered at least one resetting event. In particular, we assume the last resetting event to occur at time $t-\tau$. The probability that a resetting event occurs between time τ and $\tau + d\tau$ is $rd\tau$, which is multiplied with the probability that no resetting event occurred after $t-\tau$, which is $e^{-r\tau}$. After the last resetting event at $t = \tau$, the dynamics follows the reset-free propagator $P(x,t)$ for the remaining time τ.

A subtle point to note here is that the renewal equation (18) holds only when the full dynamics (not only the position) of the particle is reset. In our case, the friction kernel $\gamma(t)$ is a time-dependent quantity. Thus, at each resetting event, we need to restart $\gamma(t)$ to its starting value as well. That is, the memory kernel keeps the dynamics non-Markovian between the resetting intervals while the resetting event is simply Markovian. This allows us to take advantage of the *full renewal formalism*. This argument is also illustrated in Sec. V, where we discuss the simulation schemes. Let us now find the exact form of the MSD and correlation function discussed earlier in the presence of stochastic resetting.

A. MSD in the presence of resetting

The MSD in the presence of resetting is given by

$$\sigma_r^2(t) = \langle x^2(t)\rangle_r - \langle x(t)\rangle_r^2 = \int_{-\infty}^{\infty} dx\, x^2 P_r(x,t) - \left(\int_{-\infty}^{\infty} dx\, x\, P_r(x,t)\right)^2, \tag{19}$$

where $\langle x(t)\rangle_r$ and $\langle x^2(t)\rangle_r$ are the mean and second moment of position, respectively, in the presence of resetting. We can now use Eq. (18) to obtain a renewal equation for the MSD under resetting[44,45] as

$$\sigma_r^2(t) = e^{-rt}\sigma^2(t) + r\int_0^t d\tau\, e^{-r\tau}\sigma^2(\tau), \tag{20}$$

where $\sigma^2(t) = \int_{-\infty}^{\infty} dx x^2 P(x,t) - \left(\int_{-\infty}^{\infty} dx x P(x,t)\right)^2$ is the MSD of the underlying process as already found in Eq. (17). Finally, plugging the result from Eq. (17) in Eq. (20), we obtain the exact formula for MSD with resetting given as

$$\sigma_r^2(t) = \left(\frac{k_B T}{m}\right)\left(e^{-rt}\left[2I_0(t)-\omega^2 I_0^2(t)\right] + r\int_0^t d\tau\, e^{-r\tau}\left[2I_0(\tau)-\omega^2 I_0^2(\tau)\right]\right). \tag{21}$$

The above equation is general and it holds for any friction kernel. Since the system reaches a non-equilibrium steady state (NESS) under resetting in the long time limit, this is reflected in the MSD as well. To see this, we set $t\to\infty$ in Eq. (21). There, the first term vanishes in the long time limit and the MSD in the NESS for GLE reads

$$\left(\sigma_r^2\right)_{ss} = \sigma_r^2(t\to\infty) = \left(\frac{k_B T r}{m}\right)\left[2\widetilde{I}_0(r)-\omega^2\widetilde{I}_0^2(r)\right], \tag{22}$$

where recall that $\widetilde{I}_0(r)$ is the Laplace transform of $I_0(t)$ and $\widetilde{I}_0^2(r)$ denotes the Laplace transform of $I_0^2(t)$ with variable r. Note that the MSD as in Eq. (21) [or Eq. (22)] is completely independent of the initial position x_0, which is also the resetting position. Evidently, one is free to choose either a fixed value of x_0 or a random value drawn from a distribution. In addition, when the initial position and the resetting position are not exactly the same but drawn

independently from a distribution, this argument does not hold and one needs a separate renewal equation for $P_r(x,t)$. For brevity, we will focus our analysis pertaining to a fixed initial/resetting coordinate. In addition to the MSD, one can also try to extract information about the autocorrelation function of the GLE under resetting. For this purpose, one needs to write a separate renewal equation for the autocorrelation function itself. In Sec. III B, we proceed to illustrate the same.

B. Correlation function with resetting

The autocorrelation function for resetting systems has been studied recently in the context of diffusion[57] and fractional Brownian motion[58] and geometric Brownian motion.[59] In here, we adapt the renewal structure that was proposed in Ref. 59. For brevity, we briefly revisit the derivation in below. The autocorrelation function of $x(t)$ under resetting dynamics is defined in the following way: $C_r(t,t') = \langle x(t)x(t')\rangle_r$, which satisfies the following renewal relation for $t > t'$:

$$C_r(t,t') = e^{-rt}C(t,t') + r\int_0^{t'} d\tau\, e^{-r(t-t'+\tau)}C(\tau, t-t'+\tau) + r\int_0^{t-t'} d\tau\, e^{-r\tau}\langle x(t')\rangle_r\langle x(\tau)\rangle. \quad (23)$$

The renewal structure of Eq. (23) can be interpreted as follows. The first term on the RHS of Eq. (23) accounts for those trajectories, which did not undergo any resetting event for the entire observation window $[0,t]$—this survival probability is given by e^{-rt} and then it should be multiplied with $C(t,t')$, i.e., the correlation function of the underlying process. The other possibility is to have multiple resetting events prior to the interval $[t',t]$ [see Fig. 2(a)]. Let us assume that the last resetting event had happened τ amount of time before t', i.e., at the time instant $t'-\tau$. Starting from here, the motion of the particle renews. As a consequence, the correlation between t' and t is effectively the same as the correlation between τ and $t-(t'-\tau)$ measured with respect to $t'-\tau$ as the new time origin. After $t'-\tau$, no resetting event takes place for the remaining time $t-t'+\tau$ with probability $e^{-(t-t'+\tau)}$. Moreover, the probability that a resetting event occurs between time $t'-\tau$ and $t'-\tau+d\tau$ is simply $rd\tau$. Both these factors are multiplied to the underlying process's correlation function between τ and $t-t'+\tau$ where no resetting event occurs. Since τ can occur any time between 0 to t', we integrate this time out to arrive at the second term in Eq. (23). Finally, the contribution to the third term in Eq. (23) comes from the trajectories that undergo the last resetting event inside the interval $[t',t]$ [see Fig. 2(b)]. Suppose the last resetting occurs at τ time before t, i.e., at time $t-\tau$. In that case, the correlation at t' and t are simply the product of the individual expectation value of the position, since a resetting has occurred in between and there is no preceding memory. The mean position of the particle under resetting at t' is given by $\langle x(t')\rangle_r$ and it is multiplied with the $\langle x(\tau)\rangle$ during which no resetting takes place. The probability of having no resetting for the time τ after the last resetting event is simply $e^{-r\tau}$. All these quantities give rise to the third term in Eq. (23). However, for our convenience, we set $x_0 = 0$ resulting in both $\langle x(\tau)$ and $\langle x(t)\rangle_r$ to zero as well. Thus, for our case, the third term drops out and we have

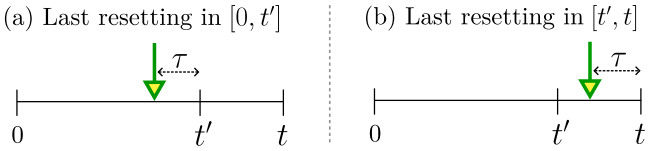

FIG. 2. A simple schematic illustrating the contribution to the correlation function from two different scenarios depending on the event of the last resetting (shown by the arrow). In (a), the last resetting happens in $[0,t']$, whereas in (b), the last resetting happens in $[t',t]$.

$$C_r(t,t') = e^{-rt}C(t,t') + r\int_0^{t'} d\tau\, e^{-r(t-t'+\tau)}C(\tau, t-t'+\tau). \quad (24)$$

The relation equation (24) is quite useful since by simply plugging the correlation function of the underlying process as in Eq. (16), one can obtain the same under resetting. To proceed to the exact evaluation of MSD [Eq. (21)] and correlation function [Eq. (24)], one requires a specific choice of the kernel $\gamma(t)$ (and, hence, the relaxation functions). In what follows, we illustrate our general results by taking an example of the Jeffreys fluid model, which has been a paradigmatic choice to model viscoelastic systems.

IV. JEFFREYS FLUID AS A VISCOELASTIC BATH

The Jeffreys fluid model has been found to be a good representation of a viscoelastic bath in several experimental systems.[24–27,29,60] It is also an intuitive yet illustrative model that can capture both the viscous and elastic timescales of the bath. The viscous part is given by the delta-correlated kernel and the elastic part is given by a mono-exponential function. This makes the model tractable analytically and by numerical simulations.

The friction kernel $\gamma(t)$ in the Jeffreys fluid model is usually considered in the following manner:[24–27,29,60]

$$\gamma(t) = 2\gamma_f\delta(t) + \frac{\gamma_s}{\tau_s}\exp\left(-\frac{t}{\tau_s}\right). \quad (25)$$

Here, the parameter γ_f relates the viscous property of the bath to the particle under consideration. The other parameters in the exponential, i.e., γ_s and τ_s determine the elastic properties of the fluid. A larger value of τ_s implies that the particles of the fluid relax very slowly, whereas γ_s measures the strength of the relaxation dynamics of the fluid in the particle's dynamics. In the limit of $\gamma_s = 0$, one recovers the result for usual Langevin dynamics with diffusion constant $D = \frac{k_BT}{m\gamma_f}$.

To move forward, we take the Laplace transform of Eq. (25) resulting in $\widetilde{\gamma}(s) = \gamma_f + \frac{\gamma_s}{1+s\tau_s}$. Using the above in Eq. (9), we find

$$\widetilde{I}_0(s) = \frac{s^{-1}}{s\left(\gamma_f + \frac{\gamma_s}{1+s\tau_s}\right) + \omega^2}, \quad (26)$$

which upon Laplace inversion yields

$$I_0(t) = \frac{1}{\omega^2}\left(1 - e^{-\alpha t/\tau_s}\cosh\left[\frac{t}{\tau_s}\sqrt{\alpha^2-\beta^2}\right] - \frac{\alpha-\beta^2}{\sqrt{\alpha^2-\beta^2}}e^{-\alpha t/\tau_s}\sinh\left[\frac{t}{\tau_s}\sqrt{\alpha^2-\beta^2}\right]\right), \quad (27)$$

where we have defined the following dimensionless quantities:

$$\alpha = \frac{\gamma_f + \gamma_s + \omega^2\tau_s}{2\gamma_f}, \quad \beta = \sqrt{\frac{\omega^2\tau_s}{\gamma_f}}. \quad (28)$$

It is now straightforward to plug this expression in Eqs. (21) and (24) to get the results for MSD and correlation function with resetting, respectively.

A. MSD

In the following, we elaborate in detail about behavior and different timescales arising in the expression of MSD in both the reset-free and resetting induced process. Let us start with the reset-free process first.

1. Underlying reset-free process

Combining Eq. (27) with Eq. (17), one obtains the exact expression for the MSD of the underlying process given by

$$\sigma^2(t) = \frac{k_BT}{m\omega^2}\left[1 - e^{-\frac{2\alpha t}{\tau_s}}\cosh^2\left(\sqrt{\alpha^2-\beta^2}t/\tau_s\right) \times \left\{1 + \left(\frac{\alpha-\beta^2}{\sqrt{\xi}}\right)\tanh\left(\sqrt{\alpha^2-\beta^2}t/\tau_s\right)\right\}^2\right]. \quad (29)$$

Figure 3 depicts the MSD of a particle following GLE for various values of γ_s. First note that, for $\gamma_s = 0$, we obtain

$$\sigma^2(t) = \frac{k_BT}{m\omega^2}\left(1 - e^{-\frac{2t\omega^2}{\gamma_f}}\right), \quad (30)$$

which is the MSD of the classical Ornstein–Uhlenbeck (OU) process. The MSD increases linearly, i.e., $\sigma^2(t) \sim \frac{2k_BTt}{m\gamma_f}$ at short times (i.e., $t \ll \gamma_f/\omega^2$). At large enough times (i.e., $t \gg \gamma_f/\omega^2$), the system reaches the *equilibrium stationary state* in a harmonic potential and the MSD saturates to $\sigma^2(t) \sim \frac{k_BT}{m\omega^2}$.

The memory in the system is introduced through the exponential term in the friction kernel Eq. (25), i.e., when γ_s is non-zero. From Fig. 3, note that an intermediate saturation region appears in the MSD due to the effects of memory ($\gamma_s \neq 0$) in GLE compared to the standard Langevin equation ($\gamma_s = 0$). The MSD increases linearly, then saturates to an intermediate plateau, then increases again, and eventually saturates to the steady state value. In what follows, we find the exact timescales showing the crossover between these distinct regimes and then extract the exact asymptotic behavior of the MSD in all of these regions. Throughout the calculations, we shall set $k_BT/m = 1$ since it is just a multiplicative factor in the expression for MSD.

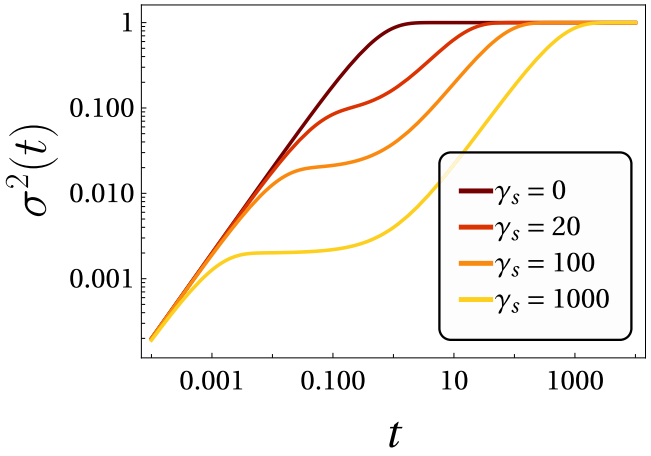

FIG. 3. MSD of the underlying reset-free process for the Jeffreys fluid model as a function of time [Eq. (29)] for different values of γ_s. For $\gamma_s = 0$, the MSD is the same as that of an OU process. The plots indicate the existence of two distinct time scales for a non-zero value of γ_s with the emergence of a plateau. In Fig. 4, we discuss the origin of these characteristics and illustrate further. The parameters for this simulation are set at: $\gamma_f = 1, \omega = 1, \tau_s = 1$.

The analysis becomes simpler when we set $\omega = 0$. The effect of ω only shows up at very large timescales when the particle starts to feel the effect of the trap and MSD begins to saturate. At short times, ω does not play any significant role in determining the MSD. Consequently, at short enough time, the results with $\omega = 0$ and $\omega \neq 0$ match quite well (see Fig. 4).

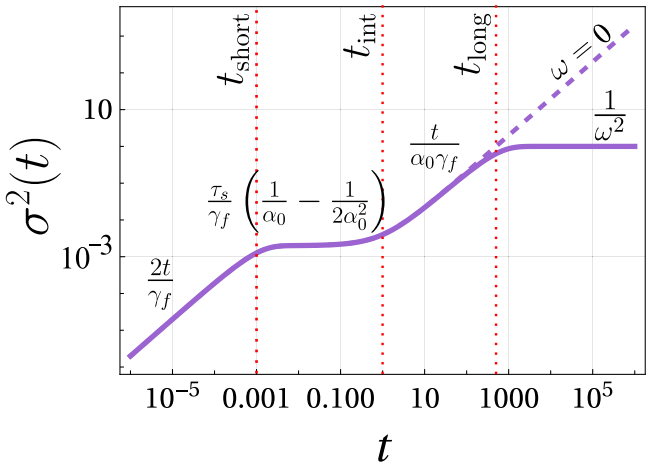

FIG. 4. Variation of the MSD of the underlying process (the solid line) as a function of time and emergence of the plateaus for parameters fixed at $\gamma_s = 1000$, $\gamma_f = 1, \omega = 1,$ and $\tau_s = 1$. This is the bottom-most curve for the MSD as borrowed from Fig. 3. The vertical dotted lines represent three different timescales as in Eqs. (33), (37), and (41). The asymptotic behavior of the MSD at different timescales is also shown above the curve in each region. The dashed line shows the MSD with $\omega = 0$ as in Eq. (32).

a. The case without potential ($\omega = 0$). Taking $\omega \to 0$ is equivalent to $\beta \to 0$ as can be seen from the expression for $\beta = \sqrt{\frac{\omega^2 \tau_s}{\gamma_f}}$ [also given in Eq. (28)] and α becomes

$$\alpha_0 = \alpha(\omega \to 0) = \frac{\gamma_f + \gamma_s}{2\gamma_f}. \tag{31}$$

In this case, the MSD takes a comparatively simpler form given by

$$\sigma^2(t)_{w\to 0} = \frac{\tau_s}{\gamma_f}\left(\frac{1}{\alpha_0} - \frac{1}{2\alpha_0^2}\right) + \frac{t}{\alpha_0\gamma_f} - e^{-2t\alpha_0/\tau_s}\frac{\tau_s}{\gamma_f}\left(\frac{1}{\alpha_0} - \frac{1}{2\alpha_0^2}\right). \tag{32}$$

The above equation has two timescales rooted inside. The short time behavior of this MSD can be obtained when $t \ll \frac{\tau_s}{2\alpha_0}$ and expanding the exponential in the last term. Evidently, the shortest timescale t_{short} in the system is given by

$$t_{\text{short}} = \frac{\tau_s}{2\alpha_0}. \tag{33}$$

In this limit, one can find

$$\sigma^2(t)_{w\to 0} \approx \frac{2t}{\gamma_f}, \quad \text{when } t \ll t_{\text{short}}. \tag{34}$$

Note that any signature of the exponential term in the kernel is absent here and the MSD grows linearly with an effective diffusion constant $D = \frac{1}{\gamma_f}$ as is also observed in Fig. 3. In contrast, when $t \gg t_{\text{short}}$, one can neglect the exponential term in Eq. (32), which yields the following result:

$$\sigma^2(t)_{w\to 0} \approx \frac{\tau_s}{\gamma_f}\left(\frac{1}{\alpha_0} - \frac{1}{2\alpha_0^2}\right) + \frac{t}{\alpha_0\gamma_f}, \text{ when } t \gg t_{\text{short}}. \tag{35}$$

The above result further shows distinct behaviors below and above an intermediate timescale t_{int}. To find this intermediate timescale, let us rewrite the expression in the following way:

$$\begin{aligned}\sigma^2(t)_{w\to 0} &\approx \frac{\tau_s}{\gamma_f}\left(\frac{1}{\alpha_0} - \frac{1}{2\alpha_0^2}\right)\left[1 + \frac{t}{\tau_s\left(1 - \frac{1}{2\alpha_0}\right)}\right] \\ &\approx \frac{\tau_s}{\gamma_f}\left(\frac{1}{\alpha_0} - \frac{1}{2\alpha_0^2}\right)\left[1 + \frac{t}{t_{\text{int}}}\right].\end{aligned} \tag{36}$$

Evidently, the intermediate timescale is given by

$$t_{\text{int}} = \tau_s\left(1 - \frac{1}{2\alpha_0}\right). \tag{37}$$

When $t \ll t_{\text{int}}$, the second time-dependent term in Eq. (36) can be neglected and the MSD attains the saturation value,

$$\sigma^2(t)_{w\to 0} \approx \frac{\tau_s}{\gamma_f}\left(\frac{1}{\alpha_0} - \frac{1}{2\alpha_0^2}\right), \text{ when } t_{\text{short}} \ll t \ll t_{\text{int}}. \tag{38}$$

The above result gives the analytical expression for the first plateau as is seen in Fig. 3. On the other hand, when $t \gg t_{\text{int}}$, we can neglect the constant value of unity in the third parenthesis of Eq. (36) to have

$$\sigma^2(t)_{w\to 0} \approx \frac{t}{\alpha_0\gamma_f}, \quad \text{when } t \gg t_{\text{int}}. \tag{39}$$

Thus, the MSD grows linearly after the intermediate region ends as also seen in Fig. 3. Let us now examine the case with $\omega \neq 0$.

b. The case with potential ($\omega \neq 0$). To find the longest timescale t_{long}, we first note that the MSD saturates to the *equilibrium* steady state value $1/\omega^2$ at long enough times $t \gg t_{\text{long}}$. This result can be verified by taking the limit $t \to \infty$ in the expression for MSD in Eq. (29). However, one can also find the correction to this term in the limit $t \to \infty$, the approximate expression for which is found to be

$$\sigma^2(t \to \infty) \approx \frac{1}{\omega^2} - A\, e^{-\frac{2t\left(\alpha - \sqrt{\alpha^2 - \beta^2}\right)}{\tau_s}}, \tag{40}$$

where A is a time-independent prefactor dependent on α, β, τ_s, and ω. The above asymptotic expression for the MSD immediately reveals the longest timescale t_{long} of the system, which is given by

$$t_{\text{long}} = \frac{\tau_s}{2\left(\alpha - \sqrt{\alpha^2 - \beta^2}\right)}. \tag{41}$$

Beyond this timescale, the MSD saturates to the steady state value. Finally, combining all of the above results, we have the MSD of the underlying system at different timescales given by (with $\frac{k_B T}{m} = 1$),

$$\sigma^2(t) \approx \begin{cases} \frac{2t}{\gamma_f}, & \text{when } t \ll t_{\text{short}}, \\ \frac{\tau_s}{\gamma_f}\left(\frac{1}{\alpha_0} - \frac{1}{2\alpha_0^2}\right), & \text{when } t_{\text{short}} \ll t \ll t_{\text{int}}, \\ \frac{t}{\alpha_0\gamma_f}, & \text{when } t_{\text{long}} \gg t \gg t_{\text{int}}, \\ \frac{1}{\omega^2}, & \text{when } t \gg t_{\text{long}}. \end{cases} \tag{42}$$

To illustrate these timescales, we select the bottom-most plot in Fig. 3 and plot it separately in Fig. 4. Here, the parameters are fixed at $\gamma_s = 1000, \gamma_f = 1, \omega = 1, \tau_s = 1$, so that $\alpha = 501, \alpha_0 = 500.5$, and $\beta = 1$. In Fig. 4, we show the different timescales of the system and the asymptotic behavior of the MSD in each of this region. Note that the plot with $\omega = 0$ shown by the dashed line matches exactly with the plot for $\omega \neq 0$ at $t \ll t_{\text{long}}$, which validates our earlier assumption.

2. Resetting induced process

Let us now delve into the details of MSD under stochastic resetting. Plugging Eq. (27) into Eq. (21) gives the exact expression for the MSD under resetting. The expression is quite lengthy and not very insightful so we have moved that to the Appendix [in particular, Eq. (A1)]. In Fig. 5, we show its behavior with respect to time. The dashed line in Fig. 5 represents the MSD without resetting. First note that resetting introduces another extra timescale

$$t_r = 1/r \tag{43}$$

in the system which is the average waiting time between two resetting intervals. Note that this timescale is independent of the system

and entirely controlled externally. From Fig. 5, it is evident that the effects of resetting show up only at the longest timescale of the system. After expanding the expression for MSD with resetting as given in Eq. (A1) in the limit $t \to \infty$, one finds

$$\sigma_r^2(t \to \infty) \approx (\sigma_r^2)_{ss} - B\, e^{-\frac{t\left(2\alpha - 2\sqrt{\alpha^2-\beta^2}+r\tau_s\right)}{\tau_s}}, \tag{44}$$

where $(\sigma_r^2)_{ss}$ is the steady state MSD under resetting given by

$$(\sigma_r^2)_{ss} = \frac{2\beta^2\left[4\alpha\,(r\tau_s+1) + r\tau_s\left(1 + r\tau_s - \beta^2\right)\right]}{\omega^2\,(2\alpha + r\tau_s)\,[4\beta^2 + r\tau_s\,(4\alpha + r\tau_s)]}, \tag{45}$$

and B is just a time-independent constant. As a consistency check, note that in the limit $r \to 0$, one finds $\left(\sigma^2_{r\to 0}\right)_{ss} = 1/\omega^2$, which was also obtained earlier. It should be noted that the steady state under resetting is not a pure equilibrium as the probability current due to resetting continuously flows through the system even at large times. Thus, this saturation value of the MSD is qualitatively distinct from the same under equilibrium conditions imposed by the harmonic trap. From Eq. (44), one can infer the longest timescale of the system under resetting t^r_{long} given as

$$t^r_{\text{long}} = \frac{\tau_s}{2\left(\alpha - \sqrt{\alpha^2-\beta^2}\right) + r\tau_s}. \tag{46}$$

When the resetting rate is very low so that $\frac{1}{r} \gg \frac{\tau_s}{2\left(\alpha-\sqrt{\alpha^2-\beta^2}\right)}$ or $t_r \gg t_{\text{long}}$, the term $r\tau_s$ in the denominator of Eq. (46) can be neglected and we have $t^r_{\text{long}} \approx t_{\text{long}}$. Thus, the steady state with or without resetting is obtained at the same timescale, although the exact steady state values of the MSD in both cases are different.

In turn, for a suitably finite value of resetting rate r, one has $t^r_{\text{long}} < t_{\text{long}}$. Hence, the steady state with resetting occurs at a time earlier than the longest timescale of the underlying process. Note that at very short times $t \ll t^r_{\text{long}}$, the effect of resetting does not show up in the system and the MSD merges with the underlying process as can be seen in Fig. 5. When the resetting rate is too high, one can neglect the first term in the denominator of Eq. (46) that results in $t^r_{\text{long}} \approx t_r = 1/r$. Steady state is obtained at times $t \gg t_r$ as evident from Fig. 5. As the effect of resetting is absent below t_r, all other timescales of the underlying process remain intact (plot with $r = 0.1$ in Fig. 5).

In the limit of significantly high resetting rate so that t_r is less than either t_{int} or t_{short}, then t_r remains the dominant timescale and the other ones vanishes. As an illustrative example, consider the curve in Eq. (5) with $r = 10$. Here, the resetting timescale $t_r = 0.1$ is shorter than the intermediate timescale $t_{\text{int}} = 1$. As a result, the intermediate timescale does not show up in the MSD and further causes the intermediate plateau to diminish. Here, the steady state is obtained just after $t_r = 0.1$, which is much earlier than t_{int}. For a sufficiently high resetting rate, one obtains the following value for the steady state MSD:

$$\left(\sigma^2_{r\to\infty}\right)_{ss} = \frac{1}{\gamma_f r}, \tag{47}$$

which is the same for a free Brownian particle with diffusion constant $D = \frac{1}{\gamma_f}$.[33]

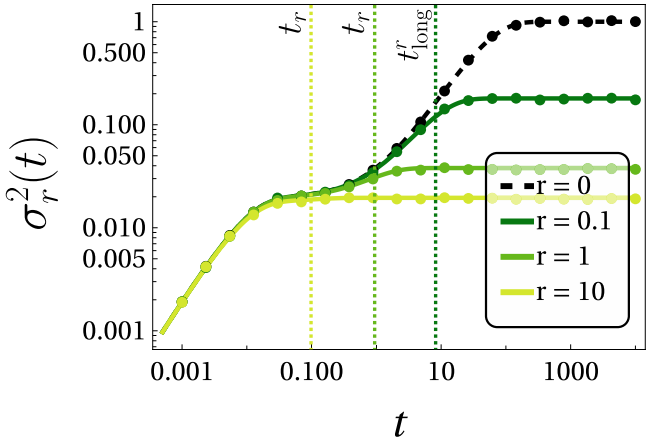

FIG. 5. Variation of MSD with time for the resetting system [see Eq. (A1)] for different values of resetting rate r. The parameters are fixed at $\gamma_f = 1$, $\gamma_s = 100$, $\tau_s = 1$, and $\omega = 1$. The circles represent the results from the simulation. The dashed curve represents the result for the underlying reset-free process, i.e., $r = 0$. The solid circles represent the results from numerical simulation. The rightmost vertical dashed line represents the longest timescale of the system under resetting while the other two vertical dashed lines are associated with the timescales t_r for different values of r (color-codes represent the values of r, respectively). At sufficiently short times $t \ll t_r, t^r_{\text{long}}$, the curves follow the MSD of the underlying reset-free process.

B. Correlation function

We now turn our attention to the analysis of the correlation function in the Jeffreys fluid model with initial position $x_0 = 0$. Plugging Eq. (27) in Eq. (16) gives us the correlation function for the underlying reset-free process. At large enough times, specifically in the limit $t \gg t' \gg \frac{\tau_s}{2\sqrt{\alpha^2-\beta^2}}$, the underlying process's correlation function becomes stationary and decays exponentially with $t - t'$ as

$$C(t, t';\, t \gg t') \sim e^{-\frac{\left(\alpha-\sqrt{\alpha^2-\beta^2}\right)(t-t')}{\tau_s}}, \tag{48}$$

where recall that $\alpha = \frac{\gamma_f+\gamma_s+\tau_s\omega^2}{2\gamma_f}$ and $\beta = \sqrt{\frac{\omega^2\tau_s}{\gamma_f}}$ (see the Appendix). The correlation is expected to die off as the system equilibrates. However, note that for $\omega \to 0$, the correlation function saturates to a fixed value indicating that there is no steady state as can be corroborated from Fig. 4, which displays the linear growth of MSD in time. The correlation function under resetting interrupted dynamics can be found by inserting Eq. (16) in Eq. (24) with $I_0(t)$ given by Eq. (27). The exact expression for the correlation function is provided in the Appendix. Figure 6 shows the behavior of the correlation function with respect to time t keeping $t' = 0.1$ fixed. Interestingly, the correlation function in the limit of very high t and t' $\left(\text{i.e., } t \gg t' \gg \frac{\tau_s}{2\sqrt{\alpha^2-\beta^2}}\right)$ again reaches a stationary form where the decay is solely governed by the difference $t - t'$. The asymptotic form in this

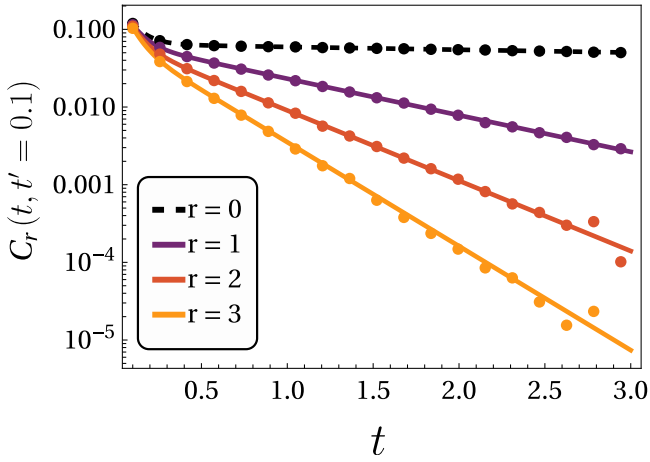

FIG. 6. Variation of the correlation function with time t under resetting for the Jeffreys fluid model [see Eq. (A3)]. We keep $t' = 0.1$ fixed. The parameters chosen are: $\gamma_f = 1, \gamma_s = 10, \omega = 1, \tau_s = 1$. As before, the dashed line represents the reset-free process ($r = 0$) and the solid circles represent data points from numerical simulation. Note that the correlation decays exponentially with time as given by Eq. (49).

limit is given by (see the Appendix for more details)

$$C_r(t, t'; t \gg t') \sim e^{-r(t-t') - \frac{\left(\alpha - \sqrt{\alpha^2 - \beta^2}\right)(t-t')}{\tau_s}}. \tag{49}$$

Notably, the correlation function under resetting vanishes in a long time as we take the $\omega \to 0$ limit. This is a manifestation of the system reaching the steady state under resetting dynamics, which was not the case for the underlying process even when the trap is turned off. Thus, resetting plays a crucial role in stabilizing the system, especially in the absence of the potential.

V. SIMULATION SCHEME FOR GLE WITH RESETTING

So far, we have focused on deriving exact results for the MSD and the correlation functions. The aim of this section is to provide the steps to solve the GLE-systems numerically. Unlike the classical Langevin equation [given by Eq. (1)], solving the GLE [given by Eq. (2)] numerically can be challenging at times as can be perceived from the earlier literature, where various simulation schemes have been proposed to handle such systems.[61–64] In this work, we follow the Markovian embedding method which has been successful in implementing non-Markovian systems especially the GLEs that represent colloids in the viscoelastic medium.[26,64–66]

It will be useful to recall the overdamped GLE for the Jeffreys fluid model as in Eq. (25), namely,

$$\gamma_f \dot{x}(t) + \frac{\gamma_s}{\tau_s} \int_0^t \exp\left(-\frac{t-t'}{\tau_s}\right) \dot{x}(t')\, dt' + \omega^2 x(t) = \xi(t), \tag{50}$$

where we have set $m = 1$. The above non-Markovian equation is difficult to solve numerically for the following reasons:

- The second term requires the storage of the velocity for all the time prior to t, which is computationally expensive. In addition, to find the time dependence of the statistical quantities, at each measurement time step, one needs to calculate the convolution of the kernel as well as the velocity upto the measurement time, which costs a significant computational time.
- Generating the noise $\xi(t)$ that has the correlation as in Eq. (3) requires the storage of correlated random numbers up to time t. For instance, to generate a single trajectory upto time t with a microscopic time interval $\Delta t = 10^{-4}$, one needs to keep track of the noise history upto time t unlike the Markovian process, where noise acts independently at each time step. So, to gather the value of MSD, say at time $t = 10^4$, one should store around $\sim 10^8$ data points of $\xi(t)$ (of approximate file size $\sim$400 MB). Now, for a better averaging with a sample set of N trajectories, one needs to generate an equal set of random numbers each containing 10^8 data points of $\xi(t)$ while running every trajectory. This task turns out to be enormously time consuming.

To circumvent these numerical hindrances, we use the Markovian embedding method which turns out to be more efficient. Below, we briefly describe this method and underpin how this evades both the problems mentioned in above.

A. Markovian embedding

To circumvent the first problem, we define an auxiliary variable $W(t)$ as

$$W(t) = \frac{\gamma_s}{\tau_s} \int_0^t \exp\left(-\frac{t-t'}{\tau_s}\right) \dot{x}(t')\, dt'. \tag{51}$$

Taking the derivative with respect to t of the above equation yields

$$\dot{W}(t) = -\frac{1}{\tau_s} W(t) + \frac{\gamma_s}{\tau_s} \dot{x}(t). \tag{52}$$

This step reduces the complexity quite a bit since the single non-Markovian equation (50) now reduces to a set of two Markovian equations as we note below

$$\begin{aligned} \dot{x} &= -\frac{1}{\gamma_f} W(t) - \frac{\omega^2}{\gamma_f} x(t) + \frac{1}{\gamma_f} \xi(t), \\ \dot{W}(t) &= -\frac{1}{\tau_s}\left(1 + \frac{\gamma_s}{\gamma_f}\right) W(t) - \frac{\omega^2}{\tau_s}\frac{\gamma_s}{\gamma_f} x(t) + \frac{1}{\tau_s}\frac{\gamma_s}{\gamma_f} \xi(t). \end{aligned} \tag{53}$$

To bypass the second problem related to the correlated noise, we define the OU process $\eta(t)$ defined as

$$\dot{\eta}(t) = -\frac{1}{\tau_s} \eta(t) + \frac{1}{\tau_s} \zeta(t), \tag{54}$$

where $\zeta(t)$ is a white noise with zero mean and correlation $\langle \zeta(t)\zeta(t')\rangle = 2\gamma_s k_B T \delta(t-t')$. Note that the correlation for an OU process $\eta(t)$ is given by

$$\langle \eta(t)\eta(t')\rangle = k_B T \frac{\gamma_s}{\tau_s} \exp\left(-\frac{|t-t'|}{\tau_s}\right). \tag{55}$$

Thus, the OU process $\eta(t)$ is able to generate the exponential correlation part as in Eq. (25). We write the noise $\xi(t)$ as

$$\xi(t) = \zeta_0(t) + \eta(t), \tag{56}$$

where $\zeta_0(t)$ is another white noise with correlation $\langle \zeta_0(t)\zeta_0(t')\rangle = 2\gamma_f k_B T\delta(t-t')$. Henceforth, we arrive at a situation where one needs to solve the following set of Markovian equations to find $x(t)$, namely,

$$\begin{aligned}\dot{x}(t) &= -\frac{1}{\gamma_f}W(t) - \frac{\omega^2}{\gamma_f}x(t) + \frac{1}{\gamma_f}\zeta_0(t) + \frac{1}{\gamma_f}\eta(t),\\ \dot{W}(t) &= -\frac{1}{\tau_s}\left(1+\frac{\gamma_s}{\gamma_f}\right)W(t) - \frac{\omega^2}{\tau_s}\frac{\gamma_s}{\gamma_f}x(t)\\ &\quad + \frac{1}{\tau_s}\frac{\gamma_s}{\gamma_f}\zeta_0(t) + \frac{1}{\tau_s}\frac{\gamma_s}{\gamma_f}\eta(t),\\ \dot{\eta}(t) &= -\frac{1}{\tau_s}\eta(t) + \frac{1}{\tau_s}\zeta(t),\end{aligned} \tag{57}$$

with the correlation of the white noises $\zeta(t), \zeta_0(t)$ given by

$$\langle \zeta(t)\zeta(t')\rangle = 2\gamma_s k_B T\delta(t-t'), \tag{58}$$

$$\langle \zeta_0(t)\zeta_0(t')\rangle = 2\gamma_f k_B T\delta(t-t'). \tag{59}$$

We mention in passing the initial condition $\vec{X}(0) = (x(0), W(0), \eta(0)) \equiv (x_0, 0, \eta_0)$, where η_0 is a randomly chosen number from the normal distribution with zero mean and variance $\sqrt{\gamma_s/\tau_s}$. At this point, we just mention that the Markovian embedding technique holds for any arbitrary kernel as well. The trick is to use the Prony series representation. Here, one represents any arbitrary function in terms of an infinite sum of exponentials. Although in that case, one may encounter an infinite number of auxiliary variables (W_i), in practice it is seen that, depending on the choice of kernel, a number of auxiliary variables as low as 7–8 can serve as a good approximation. We refer to Ref. 64 for a detailed description of the Prony series representation for an arbitrary kernel (explicitly solved for power-law kernel).

B. Stochastic resetting

Note that in our theory, resetting the particle refers to resetting both its position and the friction kernel of the viscoelastic medium back to their initial value. Consequently, to implement a resetting event, we set the particle's position along with the auxiliary variables back to the starting configuration, i.e., $\vec{X}(t) = (x(t), W(t), \eta(t)) = \vec{X}(0) \equiv (x_0, 0, \eta_0)$ at the resetting times. As each resetting event occurs at an exponentially distributed times with rate r the particle's motion at each time step Δt is governed by the following rules:

$$\vec{X}(t+\Delta t) = \begin{cases}\vec{X}(0), & \text{w.p. } r\Delta t,\\ \text{follows Eq. (57)}, & \text{w.p. } (1-r\Delta t),\end{cases} \tag{60}$$

with w.p. implying *with probability*. For the simulation, we chose $\Delta t = 10^{-4}$ and averaged the data over $\approx 10^4$ trajectories for the MSD and $\approx 10^6$ trajectories for the correlation function, respectively.

VI. DISCUSSION AND OUTLOOK

Over the last few years, stochastic resetting has gained considerable attention in the field of statistical physics, stochastic process, chemical and biological process, and in many interdisciplinary studies. These studies are carried out to their very depth in both theory[33,35,67,68] and experiments.[69–71] We refer to[34,43,72,73] for a comprehensive review of this subject. In parallel, numerous studies have successfully applied GLE with different kernels to understand the motion of biomolecules in crowded environments or colloids in an elastic medium.[15–17] This work is a first step to merge both fields and unravel the statistical properties of the GLE under stochastic resetting, and it attempts to render useful insights similar to the paradigm of diffusion under resetting.

To begin with, we extended the standard renewal formalism to accommodate Langevin systems with memory. This allowed us to derive exact expressions for the MSD and correlation function of a resetting particle in a viscoelastic medium with an arbitrary friction kernel. These generalized results are illustrated for the Jeffreys fluid model. While the MSD without resetting under the Jeffreys fluid model shows an intermediate saturation region, which is a fingerprint of the slow relaxation timescale of the viscoelastic bath, our work shows that resetting can harness this saturation region, and for a very high resetting rate, the particle is seen to effectively follow the classical diffusive behavior. In addition, we find that the correlation function decays faster in the presence of resetting. We corroborate our theoretical findings with numerical simulations of the GLE under resetting, using the Markovian embedding approach.

We believe that this work will open several future research avenues. One immediate next step would be to treat the same problem for a different kernel (e.g., power law, which is ubiquitous in anomalous diffusion phenomena[53,74–78]) and see the effect of resetting pertaining to the steady state properties. Moreover, there has been substantial advancement in recent time going beyond Markovian resetting strategies,[56,79–82] and with the inclusion of practically feasible space–time coupled resetting[83–87]—understanding these ramifications on the current system of interest would be the next promising step. In particular, the fate of the transient states at long times under power-law resetting[88] will be an interesting avenue to explore in viscoelastic systems. Furthermore, it would also be intriguing to see how the first-passage statistics in viscoelastic baths are affected in the presence of resetting. Specifically, there has been growing interest in the escape kinetics under double-well potentials.[89–92] Another interesting topic could be the influence of resetting on the particle dynamic governed by a generalized Langevin equation with exponential memory kernel in the presence of double-well potential, including the corresponding anomalous dynamics.[93] Finally, recent experiments using optical traps and colloids in the viscoelastic medium have reported ample interesting properties related to the transport properties or stochastic energetics.[26,27,29,30] It will be worthwhile to verify some of our results under resetting dynamics using these precision experiments.

ACKNOWLEDGMENTS

We are thankful to Biswajit Das for fruitful discussion and providing useful references on the methods of simulations for solving GLE. The numerical calculations reported in this work were carried out on the Nandadevi and Kamet cluster, which are maintained and supported by the Institute of Mathematical Science's High-Performance Computing Center. A.P. gratefully acknowledges research support from the Department of Atomic Energy,

Government of India via Soft Matter Apex projects. T.S. acknowledges financial support by the German Science Foundation (DFG, Grant No. ME 1535/12-1) and by the Alliance of International Science Organizations (Project No. ANSO-CR-PP-2022-05). T.S. was also supported by the Alexander von Humboldt Foundation. We thank the anonymous reviewers for many useful comments on the manuscript.

AUTHOR DECLARATIONS

Conflict of Interest

The authors have no conflicts to disclose.

Author Contributions

Arup Biswas: Conceptualization (equal); Data curation (lead); Formal analysis (lead); Investigation (lead); Methodology (equal); Validation (lead); Writing – original draft (lead); Writing – review & editing (equal). **Johan L. A. Dubbeldam:** Formal analysis (supporting); Investigation (supporting); Methodology (supporting); Writing – original draft (supporting); Writing – review & editing (supporting). **Trifce Sandev:** Conceptualization (equal); Formal analysis (supporting); Investigation (supporting); Methodology (equal); Supervision (supporting); Writing – original draft (supporting); Writing – review & editing (equal). **Arnab Pal:** Conceptualization (equal); Formal analysis (supporting); Investigation (supporting); Methodology (equal); Supervision (lead); Writing – original draft (supporting); Writing – review & editing (equal).

DATA AVAILABILITY

The data that support the findings of this study are available within the article.

APPENDIX: EXACT EXPRESSIONS FOR THE MSD AND CORRELATION FUNCTION

In this section, we provide the exact analytical expression for the MSD with resetting, i.e., $\sigma_r^2(t)$ (plotted in Fig. 5) and the correlation function both with and without resetting, i.e., $C_r(t,t')$ (plotted in Fig. 6) respectively, for Jeffrey's fluid model. In both the expressions, we assume $k_BT/m = 1$. With α, β defined as in Eq. (28), the MSD with resetting is given by

$$\sigma_r^2(t) = \frac{\beta^2}{\omega^2(\alpha^2-\beta^2)\left(4\beta^2 + r\tau_s\left(4\alpha + r\tau_s\right)\right)}\Bigg[e^{-t\left(r+\frac{2\alpha}{\tau_s}\right)}\Bigg(\sqrt{\alpha^2-\beta^2}\left(-4\alpha+4\beta^2+\left(\beta^2-1\right)r\tau_s\right)\sinh\left(\frac{2t\sqrt{\alpha^2-\beta^2}}{\tau_s}\right)$$
$$-\left(4\alpha^2-2(2\alpha+1)\beta^2+2\beta^4+r\left((\alpha-2)\beta^2+\alpha\right)\tau_s\right)\cosh\left(\frac{2t\sqrt{\alpha^2-\beta^2}}{\tau_s}\right)\Bigg)$$
$$+\frac{2(\alpha^2-\beta^2)\left(4\alpha+r\tau_s\left(4\alpha-\beta^2+r\tau_s+1\right)\right)-\alpha\left(2\alpha-\beta^2-1\right)\left(4\beta^2+r\tau_s\left(4\alpha+r\tau_s\right)\right)e^{-t\left(r+\frac{2\alpha}{\tau_s}\right)}}{2\alpha+r\tau_s}\Bigg]. \tag{A1}$$

The correlation function of the underlying process, i.e., $C(t,t')$ for $t > t'$ is given by

$$C(t,t') = \frac{e^{-\frac{\alpha(t'+t)}{\tau_s}}}{2\omega^2(\alpha^2-\beta^2)}\Bigg(\left(\beta^2\left(-2\alpha+\beta^2+1\right)+2\alpha^2-\beta^2e^{\frac{2\alpha t'}{\tau_s}}\right)\cosh\left(\frac{\sqrt{\alpha^2-\beta^2}(t-t')}{\tau_s}\right)$$
$$+\left(-2\alpha^2+2\alpha\beta^2-\beta^4+\beta^2\right)\cosh\left(\frac{\sqrt{\alpha^2-\beta^2}(t'+t)}{\tau_s}\right)$$
$$-2\sqrt{\alpha^2-\beta^2}\left(\alpha-\beta^2\right)\left(\sinh\left(\frac{\sqrt{\alpha^2-\beta^2}(t'+t)}{\tau_s}\right)-e^{\frac{2\alpha t'}{\tau_s}}\sinh\left(\frac{\sqrt{\alpha^2-\beta^2}(t-t')}{\tau_s}\right)\right)\Bigg). \tag{A2}$$

The correlation function under resetting, after utilizing Eqs. (16) and (24), is given by

$$C_r(t,t') = \frac{e^{-r(t-t')}}{2\omega^2(\beta^2-\alpha^2)\left(4\beta^2+r\tau_s\left(4\alpha+r\tau_s\right)\right)}\Bigg(\frac{r\tau_s\,e^{-rt'-\frac{\alpha(t'+t)}{\tau_s}}\cosh\left(\frac{-\sqrt{\alpha^2-\beta^2}(t-t')}{\tau_s}\right)}{2\alpha+r\tau_s}$$
$$\times\left[\beta^2\left(-2\alpha+\beta^2+1\right)\left(4\beta^2+r\tau_s\left(4\alpha+r\tau_s\right)\right)+2(\alpha^2-\beta^2)\left(2\left(\left(\beta^2-2\alpha\right)^2+\beta^2\right)+r\tau_s\left(6\alpha-2\beta^2+r\tau_s\right)\right)e^{t'\left(r+\frac{2\alpha}{\tau_s}\right)}\right]$$

$$+ e^{-3rt'-\frac{\alpha(3t'+t)}{\tau_s}}\left[-e^{2t'\left(r+\frac{\alpha}{\tau_s}\right)}\left(\beta^2\left(-2\alpha+\beta^2+1\right)+2(\alpha^2-\beta^2)e^{t'\left(r+\frac{2\alpha}{\tau_s}\right)}\right)\cosh\left(\frac{\sqrt{\alpha^2-\beta^2}(t-t')}{\tau_s}\right)\right.$$
$$\times\left(4\beta^2+r\tau_s\left(4\alpha+r\tau_s\right)\right)+2\beta^2\left[e^{2t'\left(r+\frac{\alpha}{\tau_s}\right)}\cosh\left(\frac{\sqrt{\alpha^2-\beta^2}(t'+t)}{\tau_s}\right)\right.\left(4\alpha^2-2(2\alpha+1)\beta^2+2\beta^4+r\left((\alpha-2)\beta^2+\alpha\right)\tau_s\right)$$
$$-\sqrt{\alpha^2-\beta^2}(4\alpha-\left(\beta^2\left(r\tau_s+4\right)\right)+r\tau_s)\left[e^{3rt'+\frac{4\alpha t'}{\tau_s}}\sinh\left(\frac{\sqrt{\alpha^2-\beta^2}(t-t')}{\tau_s}\right)\right.$$
$$\left.\left.\left.-\ e^{2t'\left(r+\frac{\alpha}{\tau_s}\right)}\sinh\left(\frac{\sqrt{\alpha^2-\beta^2}(t'+t)}{\tau_s}\right)\right]\right]\right]. \tag{A3}$$

1. Asymptotic behavior of the correlation function

Let us now provide the exact asymptotic forms of the correlation function, which was discussed briefly in Sec. IV B. The exact asymptotic form of the correlation function of the underlying reset-free process is given by

$$C(t,t';\,t\gg t')\sim\frac{\exp\left(-\frac{t'\left(\sqrt{\alpha^2-\beta^2}+\alpha\right)+t\left(\alpha-\sqrt{\alpha^2-\beta^2}\right)}{\tau_s}\right)}{4\omega^2(\alpha^2-\beta^2)}\left(2\left(\alpha^2-\beta^2\left(\sqrt{\alpha^2-\beta^2}+1\right)+\alpha\sqrt{\alpha^2-\beta^2}\right)e^{\frac{2\alpha t'}{\tau_s}}\right.$$
$$\left.+\beta^2\left(-2\alpha+\beta^2+1\right)+e^{\frac{2t'\sqrt{\alpha^2-\beta^2}}{\tau_s}}\left(-2\alpha^2+2\alpha\left(\beta^2-\sqrt{\alpha^2-\beta^2}\right)+\beta^2\left(2\sqrt{\alpha^2-\beta^2}-\beta^2+1\right)\right)\right). \tag{A4}$$

Keeping t' fixed, in the limit $t\to\infty$, note that the term under the parenthesis is just a constant prefactor with the only t dependence coming through the exponential term outside, which is $e^{-\frac{\left(\alpha-\sqrt{\alpha^2-\beta^2}\right)t}{\tau_s}}$, the result provided in Eq. (48). Moreover, note that when $t'\gg\frac{\tau_s}{2\sqrt{\alpha^2-\beta^2}}$, then the first term in the parentheses of Eq. (A4) is the most dominating one, and we obtain

$$C\left(t,t';\,t\gg t'\gg\frac{\tau_s}{2\sqrt{\alpha^2-\beta^2}}\right)\sim\frac{2\left(\alpha^2-\beta^2\left(\sqrt{\alpha^2-\beta^2}+1\right)+\alpha\sqrt{\alpha^2-\beta^2}\right)}{4\omega^2(\alpha^2-\beta^2)}\exp\left\{-\frac{\left(\alpha-\sqrt{\alpha^2-\beta^2}\right)(t-t')}{\tau_s}\right\}. \tag{A5}$$

The above result implies that the correlation function of the reset-free process reaches a stationary form in the limit of very large t and t'.

On the other hand, the asymptotic behavior of the correlation function under resetting is given by

$$C_r(t,t';\,t\gg t')\sim\frac{\beta^2\exp\left(-\frac{t\left(-\sqrt{\alpha^2-\beta^2}+\alpha+r\tau_s\right)+t'\left(\sqrt{\alpha^2-\beta^2}+\alpha\right)}{\tau_s}\right)}{2\omega^2(\alpha^2-\beta^2)(2\alpha+r\tau_s)\left(4\beta^2+r\tau_s(4\alpha+r\tau_s)\right)}\left(\alpha\left(-2\alpha+\beta^2+1\right)\left(4\beta^2+r\tau_s(4\alpha+r\tau_s)\right)\right.$$
$$\times(2\alpha+r\tau_s)\,e^{\frac{2t'\sqrt{\alpha^2-\beta^2}}{\tau_s}}\left[4\alpha^2+2\beta^4+r\tau_s\sqrt{\alpha^2-\beta^2}-\beta^2\left(4\sqrt{\alpha^2-\beta^2}+r\tau_s\left(\sqrt{\alpha^2-\beta^2}+2\right)+2\right)\right.$$
$$\left.+\alpha\left(4\sqrt{\alpha^2-\beta^2}+\beta^2(r\tau_s-4)+r\tau_s\right)\right]+e^{t'\left(\frac{2\alpha}{\tau_s}+r\right)}\left[8\alpha^3(r\tau_s+1)+2\alpha^2\left(r\tau_s\left(-\beta^2+r\tau_s+1\right)-4\sqrt{\alpha^2-\beta^2}\right)\right.$$
$$+2\alpha\left(\beta^2\left(4\left(\sqrt{\alpha^2-\beta^2}-1\right)+r\tau_s\left(\sqrt{\alpha^2-\beta^2}-4\right)\right)-3r\tau_s\sqrt{\alpha^2-\beta^2}\right)$$
$$\left.\left.+r\tau_s\left(2\beta^4+\beta^2\left(4\sqrt{\alpha^2-\beta^2}+r\tau_s\left(\sqrt{\alpha^2-\beta^2}-2\right)-2\right)-r\tau_s\sqrt{\alpha^2-\beta^2}\right)\right]\right). \tag{A6}$$

For fixed t', one can again see that the only t dependent term lies outside the parenthesis and is given by $e^{-rt-\frac{\left(\alpha-\sqrt{\alpha^2-\beta^2}\right)t}{\tau_s}}$, which is Eq. (49) from the main text. Likewise, the reset-free case, one can again take the limit of both t,t' limit here too. In the limit $t'\gg\frac{\tau_s}{2\sqrt{\alpha^2-\beta^2}}$ one can again neglect the first term under the parentheses in Eq. (A6) to have

$$C_r(t,t';\, t \gg t') \sim \frac{e^{-r(t-t')-\frac{\left(\alpha-\sqrt{\alpha^2-\beta^2}\right)(t-t')}{\tau_s}}\beta^2}{2\omega^2(\alpha^2-\beta^2)(2\alpha+r\tau_s)\,(4\beta^2+r\tau_s(4\alpha+r\tau_s))}$$
$$\times\left(8\alpha^3(r\tau_s+1)+2\alpha^2\left(r\tau_s(-\beta^2+r\tau_s+1)-4\sqrt{\alpha^2-\beta^2}\right)\right.$$
$$+2\alpha\left(\beta^2\left(4(\sqrt{\alpha^2-\beta^2}-1)+r\tau_s(\sqrt{\alpha^2-\beta^2}-4)\right)-3r\tau_s\sqrt{\alpha^2-\beta^2}\right)$$
$$\left.+r\tau_s\left(2\beta^4+\beta^2\left(4\sqrt{\alpha^2-\beta^2}+r\tau_s(\sqrt{\alpha^2-\beta^2}-2)-2\right)-r\tau_s\sqrt{\alpha^2-\beta^2}\right)\right). \quad \text{(A7)}$$

Note that at large t, t', the correlation function with resetting also reaches a stationary form where it decays exponentially with $t-t'$.

REFERENCES

[1] P. Langevin, C.R. Acad. Sci. Paris **146**, 530 (1908).
[2] H. Mori, Prog. Theor. Phys. **33**, 423 (1965).
[3] R. Kubo, Rep. Prog. Phys. **29**, 255 (1966).
[4] P. Hänggi, Z. Phys. B: Condens. Matter **31**, 407 (1978).
[5] P. Häunggi and P. Jung, Adv. Chem. Phys. **89**, 239 (1994).
[6] E. Lutz, Phys. Rev. E **64**, 051106 (2001).
[7] A. D. Viñales and M. A. Desposito, Phys. Rev. E **73**, 016111 (2006).
[8] M. A. Desposito and A. D. Viñales, Phys. Rev. E **77**, 031123 (2008).
[9] S. Burov and E. Barkai, Phys. Rev. E **78**, 031112 (2008).
[10] M. A. Desposito and A. D. Viñales, Phys. Rev. E **80**, 021111 (2009).
[11] T. Sandev, Ž. Tomovski, and J. L. A. Dubbeldam, Physica A **390**, 3627 (2011).
[12] H. Yang, G. Luo, P. Karnchanaphanurach, T.-M. Louie, I. Rech, S. Cova, L. Xun, and X. S. Xie, Science **302**, 262 (2003).
[13] S. C. Kou and X. S. Xie, Phys. Rev. Lett. **93**, 180603 (2004).
[14] G. R. Kneller, J. Chem. Phys. **141**, 041105 (2014).
[15] I. Goychuk, Adv. Chem. Phys. **150**, 187 (2012).
[16] O. F. Lange and H. Grubmüller, J. Chem. Phys. **124**, 214903 (2006).
[17] H. S. Lee, S.-H. Ahn, and E. F. Darve, J. Chem. Phys. **150**, 174113 (2019).
[18] L. Lizana, T. Ambjörnsson, A. Taloni, E. Barkai, and M. A. Lomholt, Phys. Rev. E **81**, 051118 (2010).
[19] A. Taloni, A. Chechkin, and J. Klafter, Phys. Rev. Lett. **104**, 160602 (2010).
[20] J. L. A. Dubbeldam, A. Milchev, V. G. Rostiashvili, and T. A. Vilgis, Phys. Rev. E **76**, 010801(R) (2007).
[21] R. Zwanzig, *Nonequilibrium Statistical Mechanics* (Oxford University Press, 2001).
[22] K.-G. Wang and J. Masoliver, Physica A **231**, 615 (1996).
[23] S. A. Adelman, J. Chem. Phys. **64**, 124 (1976).
[24] B. R. Ferrer, J. R. Gomez-Solano, and A. V. Arzola, Phys. Rev. Lett. **126**, 108001 (2021).
[25] J. R. Gomez-Solano and C. Bechinger, New J. Phys. **17**, 103032 (2015).
[26] B. Das, S. Paul, S. K. Manikandan, and A. Banerjee, New J. Phys. **25**, 093051 (2023).
[27] S. Paul, N. Narinder, A. Banerjee, K. R. Nayak, J. Steindl, and C. Bechinger, Sci. Rep. **11**, 2023 (2021).
[28] J. R. Gomez-Solano, A. Blokhuis, and C. Bechinger, Phys. Rev. Lett. **116**, 138301 (2016).
[29] J. R. Gomez-Solano, Front. Phys. **9**, 643333 (2021).
[30] F. Darabi, B. R. Ferrer, and J. R. Gomez-Solano, New J. Phys. **25**, 103021 (2023).
[31] S. Paul, B. Roy, and A. Banerjee, J. Phys.: Condens. Matter **30**, 345101 (2018).
[32] A. V. Straube and F. Höfling, "Memory effects in colloidal motion under confinement and driving," J. Phys. A: Math. Theor. **57**(29) 295003 (2024).
[33] M. R. Evans and S. N. Majumdar, Phys. Rev. Lett. **106**, 160601 (2011).
[34] M. R. Evans, S. N. Majumdar, and G. Schehr, J. Phys. A: Math. Theor. **53**, 193001 (2020).
[35] A. Pal, Phys. Rev. E **91**, 012113 (2015).
[36] T. Sandev, V. Domazetoski, L. Kocarev, R. Metzler, and A. Chechkin, J. Phys. A: Math. Theor. **55**, 074003 (2022).
[37] W. Wang, A. G. Cherstvy, H. Kantz, R. Metzler, and I. M. Sokolov, Phys. Rev. E **104**, 024105 (2021).
[38] T. Sandev, L. Kocarev, R. Metzler, and A. Chechkin, Chaos Soliton. Fract. **165**, 112878 (2022).
[39] M. Lenzi, E. Lenzi, L. Guilherme, L. Evangelista, and H. Ribeiro, Physica A **588**, 126560 (2022).
[40] Ł. Kuśmierz and E. Gudowska-Nowak, Phys. Rev. E **99**, 052116 (2019).
[41] V. Méndez, A. Masó-Puigdellosas, and D. Campos, Phys. Rev. E **105**, 054118 (2022).
[42] V. Méndez, A. Masó-Puigdellosas, T. Sandev, and D. Campos, Phys. Rev. E **103**, 022103 (2021).
[43] A. Pal, V. Stojkoski, and T. Sandev, *Target Search Problems* (Springer, 2024), pp. 323–355.
[44] V. Méndez and D. Campos, Phys. Rev. E **93**, 022106 (2016).
[45] V. Stojkoski, T. Sandev, L. Kocarev, and A. Pal, Phys. Rev. E **104**, 014121 (2021).
[46] S. Eule and J. J. Metzger, New J. Phys. **18**, 033006 (2016).
[47] O. Tal-Friedman, Y. Roichman, and S. Reuveni, Phys. Rev. E **106**, 054116 (2022).
[48] S. Ray and S. Reuveni, J. Chem. Phys. **152**, 234110 (2020).
[49] S. N. Majumdar, S. Sabhapandit, and G. Schehr, Phys. Rev. E **91**, 052131 (2015).
[50] R. Singh, R. Metzler, and T. Sandev, J. Phys. A: Math. Theor. **53**, 505003 (2020).
[51] N. G. Van Kampen, *Stochastic Processes in Physics and Chemistry* (Elsevier, 1992), Vol. 1.
[52] S. C. Kou, Ann. Appl. Stat. **2**, 501 (2008).
[53] W. Min, G. Luo, B. J. Cherayil, S. Kou, and X. S. Xie, Phys. Rev. Lett. **94**, 198302 (2005).
[54] N. Pottier, Physica A **317**, 371 (2003).
[55] M. R. Evans and S. N. Majumdar, J. Phys. A: Math. Theor. **47**, 285001 (2014).
[56] A. Masó-Puigdellosas, D. Campos, and V. Méndez, Phys. Rev. E **99**, 012141 (2019).
[57] V. Stojkoski, T. Sandev, L. Kocarev, and A. Pal, J. Phys. A: Math. Theor. **55**, 104003 (2022).
[58] S. N. Majumdar and G. Oshanin, J. Phys. A: Math. Theor. **51**, 435001 (2018).
[59] D. Vinod, A. G. Cherstvy, R. Metzler, and I. M. Sokolov, Phys. Rev. E **106**, 034137 (2022).
[60] Y. L. Raikher, V. V. Rusakov, and R. Perzynski, Soft Matter **9**, 10857 (2013).
[61] M. H. Duong and X. Shang, J. Comput. Phys. **464**, 111332 (2022).
[62] M. Wiśniewski, J. Łuczka, and J. Spiechowicz, Phys. Rev. E **109**, 044116 (2024).
[63] N. Bockius, J. Shea, G. Jung, F. Schmid, and M. Hanke, J. Phys.: Condens. Matter **33**, 214003 (2021).
[64] A. D. Baczewski and S. D. Bond, J. Chem. Phys. **139**, 044107 (2013).
[65] P. Siegle, I. Goychuk, P. Talkner, and P. Hänggi, Phys. Rev. E **81**, 011136 (2010).
[66] P. Siegle, I. Goychuk, and P. Hänggi, Europhys. Lett. **93**, 20002 (2011).
[67] S. Gupta, S. N. Majumdar, and G. Schehr, Phys. Rev. Lett. **112**, 220601 (2014).
[68] I. M. Sokolov, Phys. Rev. Lett. **130**, 067101 (2023).
[69] O. Tal-Friedman, A. Pal, A. Sekhon, S. Reuveni, and Y. Roichman, J. Phys. Chem. Lett. **11**, 7350 (2020).
[70] B. Besga, A. Bovon, A. Petrosyan, S. N. Majumdar, and S. Ciliberto, Phys. Rev. Res. **2**, 032029 (2020).

[71] S. Paramanick, A. Biswas, H. Soni, A. Pal, and N. Kumar, PRX Life **2**, 033007 (2024).
[72] A. Pal, S. Kostinski, and S. Reuveni, J. Phys. A: Math. Theor. **55**, 021001 (2022).
[73] S. Gupta and A. M. Jayannavar, Front. Phys. **10**, 789097 (2022).
[74] F. Ginot, J. Caspers, M. Krüger, and C. Bechinger, Phys. Rev. Lett. **128**, 028001 (2022).
[75] W. Min and X. S. Xie, Phys. Rev. E: Stat. Nonlinear Soft Matter Phys. **73**, 010902 (2006).
[76] T. Sandev, A. Chechkin, H. Kantz, and R. Metzler, Fract. Calc. Appl. Anal. **18**, 1006 (2015).
[77] J. Ślęzak, R. Metzler, and M. Magdziarz, New J. Phys. **20**, 023026 (2018).
[78] A. S. Bodrova and I. M. Sokolov, Phys. Rev. E **101**, 062117 (2020).
[79] A. Pal, A. Kundu, and M. R. Evans, J. Phys. A: Math. Theor. **49**, 225001 (2016).
[80] A. Pal and S. Reuveni, Phys. Rev. Lett. **118**, 030603 (2017).
[81] M. Radice, J. Phys. A: Math. Theor. **55**, 224002 (2022).
[82] R. Singh, R. Metzler, and T. Sandev, Chaos **35**, 011103 (2025).
[83] A. S. Bodrova and I. M. Sokolov, Phys. Rev. E **101**, 052130 (2020).
[84] G. Tucci, A. Gambassi, S. N. Majumdar, and G. Schehr, Phys. Rev. E **106**, 044127 (2022).
[85] A. Biswas, A. Kundu, and A. Pal, Phys. Rev. E **110**, L042101 (2024).
[86] A. Pal, Ł. Kuśmierz, and S. Reuveni, Phys. Rev. Res. **2**, 043174 (2020).
[87] D. Gupta, C. A. Plata, A. Kundu, and A. Pal, J. Phys. A: Math. Theor. **54**, 025003 (2020).
[88] A. Nagar and S. Gupta, Phys. Rev. E **93**, 060102 (2016).
[89] Y. P. Kalmykov, W. Coffey, and S. Titov, J. Chem. Phys. **124**, 024107 (2006).
[90] L. Caprini, U. Marini Bettolo Marconi, A. Puglisi, and A. Vulpiani, J. Chem. Phys. **150**, 024902 (2019).
[91] A. Lapolla and A. Godec, J. Chem. Phys. **153**, 194104 (2020).
[92] K. Capała, B. Dybiec, and E. Gudowska-Nowak, Chaos **30**, 013127 (2020).
[93] M. Kimura and T. Akimoto, J. Chem. Phys. **159**, 055102 (2023).